
Research article

Thermo-bioconvection flow of Walter's B nanofluid over a Riga plate involving swimming motile microorganisms

M. S. Alqarni*

Department of Mathematics, College of Science, King Khalid University, Abha 61413, Saudi Arabia

* Correspondence: Email: msalqarni@kku.edu.sa.

Abstract: The novelty of the current paper is to study the bioconvection effects in Walter's B nanofluid flow due to stretchable surface, which leads to important properties, i.e., thermal radiation, activation energy, motile microorganisms and convective boundary constraints. The considered analysis is explained via partial differential equations (PDEs), which are first embedded into the dimensionless system of nonlinear ODEs through suitable transformations. The governing equations are solved in MATLAB using the bvp4c solver. The impact of interesting parameters on the velocity field, thermal field, concentration of species and concentration of microorganisms is exhibited in graphical and tabular forms. The velocity field increases for higher estimations of the modified Hartmann and mixed convection parameters. The thermal field decays for a higher magnitude of the Prandtl number, while it is enhanced for a larger deviation of the thermal conductivity parameter. The volumetric concentration of nanoparticles enhances the larger activation energy and thermophoresis parameters. The microorganism concentration diminishes for higher Peclet number. The current model is more useful in various fields such as tissue engineering, recombinant proteins, synthetic biology, and biofuel cell and drug delivery devices.

Keywords: Walter's B nanofluid; Riga plate; activation energy; variable thermal conduction and concentration diffusion; thermal radiation; swimming motile microorganisms; bioconvection; numerical solution

Mathematics Subject Classification: 35Qxx, 76Dxx, 76Mxx

Nomenclature

u, v	Velocity-components [$m.s^{-1}$]	Sn_x	Microorganism density number
x, y	Space-coordinate [m]	N_∞	Ambient-microorganism
B_0	Magnetic-field strength [$N.m^{-1}.A^{-1}$]	T_∞	Ambient-temperature [K]
$U_w(x)$	Stretching velocity [$m.s^{-1}$]	C_∞	Ambient-concentration
$(\rho c)_p$	Nanoparticles specific-heat [$J.kg^{-3}.K^{-1}$]	D_B	Brownian-diffusion coefficient [$m^2.s^{-1}$]
$(\rho c)_f$	Thermal capacity of the fluid [$J.kg^{-3}.K^{-1}$]	D_m	Microorganism-diffusion coefficient [$m^2.s^{-1}$]
T	Temperature [K]	D_T	Thermophoresis-diffusion coefficient [$m^2.s^{-1}$]
E_a	Coefficient of activation energy	K	Thermal conductivity
σ^{**}	Stefan-Boltzmann constant	k_1	Mean-absorption coefficient
ρ_p	Density of nanoparticles	ρ_m	Microorganism density
J_0	Density of the current for electrodes	ν	Kinematic-viscosity [$m^2.s^{-1}$]
h_f	Coefficient of heat transfer	c	Stretching rate
M_0	Magnetization of the permanent magnets of Riga plate	a	Distance across the magnets electrodes of Riga plate
Nc	Bioconvective Rayleigh-number	b	Chemotaxis-constant [m]
Nr	Buoyancy-ratio number	n	Fitted-rate constant
Nb	Brownian-movement number	Ω	Microorganism-difference number
B^*	Mixed-convective parameter	σ	Electrical conductivity [$S.m^{-1}$]
Nt	Thermophoretic parameter	α	Thermal-diffusivity [$m^2.s^{-1}$]
E	Activation-energy number	σ^*	Chemical-reaction number
Le	Lewis parameter	W_c	Cell-swimming-speed [$m.s^{-1}$]
We	Weissenberg parameter	ρ	Density [$kg.m^{-3}$]
Pe	Peclet-parameter	N_w	Microorganism at wall
Lb	Bioconvective Lewis parameter	T_f	Hot fluid temperature [K]
Nu_x	Nusselt number	N	Microorganism
C_f	Skin friction	Kr^2	Chemical-reaction-constant
Su_x	Sherwood number	M	Magnetic parameter
β	Dimensionless parameter	S	Velocity ratio number
δ	Heat generation/absorption parameter	Q	Modified Hartmann number
Bi	Thermal-Biot number	Rd	Thermal radiation parameter
Pr	Prandtl number	δ_0	Temperature-difference number

1. Introduction

The description of non-Newtonian fluids has fascinated the interest of various authors due to their wide variety of practical uses in various fields. Walter's B liquid is subclass of non-Newtonian liquids with several manufacturing process applications in industry sectors such as chemical science, biosystems, biophysical techniques of thermal conduction in tissues, chemical manufacturing, and bioengineering. Walters [1] was a pioneer of the Walters'-B liquid relation. Nandepanavar et al. [2] discussed the impact of nanomaterials in Walters'-B liquid. The effect of nanoparticles in the Walters-B fluid was investigated by Nadeem et al. [3]. The effect of the radiative-Walters-B liquid flow and

stretched wedge was investigated by Hayat et al. [4]. In addition, several scientists have applied the Walters-B relation, which shows the phenomenon of different polymer flows (see [5–10]).

A nanofluid is a fluid that consists of a base fluid with nanosized particles (1–100 nm) suspended in it. Thus, Choi and Eastman [11] discussed the fundamental idea of nanomaterials with enhanced thermophysical aspects. Buongiorno [12] explained seven-slipping procedures in the movement of nanomaterials, including thermophoresis and Brownian diffusion. Mixed convective nanoliquid transport with the impact of a magnetic field was observed by Hsiao [13]. Rashidi et al. [14] numerically premeditated the convection characteristics of a nanoliquid through a nonlinear isothermal stretching sheet. Sheikholeslami and Bhatti [15] identified the impact of nanomaterials on the transport of nanoliquids via forced-convection through gravitational-force. Turkyilmazoglu [16] analyzed nanomaterial transport by vertical surfaces. Ellahi et al. [17] noted Jeffrey MHD nanoliquid motion between two parallel-disks. Pantokratoras et al. [18] discussed mixed convective fluids with nanoparticles. Rashid et al. [19] deliberated the behavior of activation energy in the MHD flow of Maxwell nanoliquid. Tayebi et al. [20] explored the magnetic hydrodynamic heat-transport of nanoliquids when wave conduction rings occurred. Hayat et al. [21] discussed the third grade magnetohydrodynamic nanoliquid flow with activation-energy. Muhammad et al. [22] explored the 3D radiative Eyring-Powell nanoliquid transport in the presence of activation-energy by a Riga plate. The transport of second-order slip nanoliquids under the effect of the Stefan blow was examined by Alamri et al. [23]. Khan et al. [24] discussed the stratification and heat generation in mixed convective Prandtl liquid flow. Anwar et al. [25] observed the nonlinear radiative heat transport with MHD nanoliquid spray. Gailitis [26] developed a Riga electromagnetic surface, which comprised clearly constructed electrode and magnet sets. Ahmad et al. [27] investigated the impact of nanoliquid flow through Riga plate. The features of microorganisms in nanoliquids across Riga plate were analyzed by Iqbal et al. [28]. Recent works have experimentally explored nanofluids in [29–35].

Bioconvection resulting from the combined density gradient of the microorganism simulates macroscopic fluid convection movements. The presence of these self-contained motile microorganisms enhances the primary-density of the fluid through swimming. This important thought certainly escorts to a delicate low-density surface. There are various distinct and related properties of nanoparticles and motile microorganisms. Immunology-microsystems such as enzyme biomaterials usually include bioconvection technologies. Therefore, Kuznetsov [36] recommended that nano-organisms should be involved in the development of bio microsystems, where they played a significant role in the dispensation of mass transport. Li et al. [37] studied the bioconvective flow of second-grade nanoliquids because of Wu's slipping. Muhammad et al. [38] analyzed the influence of bioconvection in Carreau nanoliquid under slip formed by a wedge. Khan et al. [39] examined the 2-D couple stress nanoliquid transport with magnetic-field and gyrotactic motile microorganisms. The characteristics of activation energy in radiative nanoliquid flow with bioconvection features through shrinking/stretching disks were addressed by Zhang et al. [40]. Thermal radiative Oldroyd-B nanoliquid flow subject to motile microorganisms by rotating disk was examined by Waqas et al. [41]. Khan et al. [42] examined the bioconvective aspect between stretchable moving-disks subject to entropy generation and nanofluids. Mamatha et al. [43] discussed the movement of magneto-hydrodynamic liquid by a stretched surface. Ferdows et al. [44] observed the heat and mass transportation of viscous liquid via cylinder with motile microorganisms. Amirsom et al. [45] addressed the 3-D motion of bioconvection nanoliquids consisting of gyrotactic microorganisms. Kasaragadda et al. [46] illustrated the consequence of strong hydrophobic surfaces on the recognition

of structures of nanoparticle-reinforced biomaterials. Ansari et al. [47] explored the significance of motile microorganisms and biomaterials on bioconvective Casson liquid flow by a nonlinear extended boundary. Recent work on bioconvection is given in investigations [48–55].

In this paper, we generalize the analysis of [56] in four directions. First, we model the flow analysis in the presence of nanoparticles. Attention is mainly given to Brownian and thermophoretic diffusion. Second, we consider the swimming gyrotactic motile microorganisms. Third, we analyzed the concentration and temperature in the presence of variable thermal-conductivity and concentration-diffusion. Fourth, we develop the numerical solution using the MATLAB bvp4c solver, which follows the Lobatto-IIIA formula. The consequences of parameters of interest versus the flow field are presented through graphs and tabular data.

2. Mathematical modeling

The two-dimensional magnetohydrodynamic flow of Walter's B nanoliquid containing gyrotactic motile microorganisms configured by a Riga plate in the occurrence of variable thermal conduction and concentration diffusion is considered. Features of heat generation/absorption and Arrhenius activation energy are also accounted for in the considered flow problems. The movement of fluid is caused by a stretchable surface. The features of thermal radiation are employed. The significance of Brownian and thermophoresis movements is considered. The physical flow configuration is depicted in Figure 1.

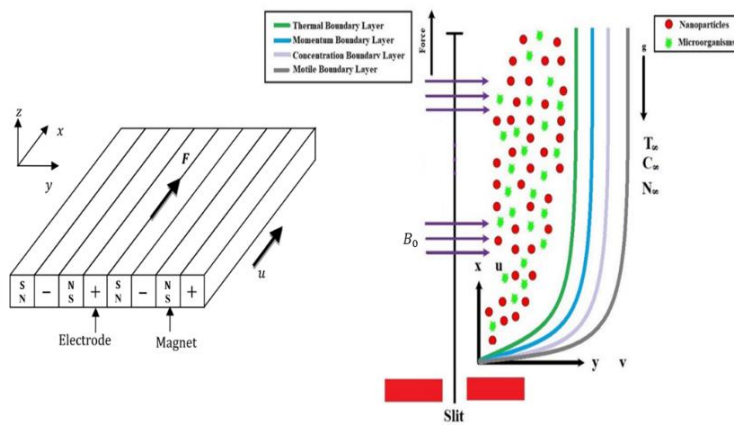


Figure 1. Physical description of the current problem.

Based on these assumptions, the governing expressions and boundary constraints are given as [1,28,55]:

$$\frac{\partial u}{\partial x} + \frac{\partial v}{\partial y} = 0, \quad (1)$$

$$u \frac{\partial u}{\partial x} + v \frac{\partial u}{\partial y} = U_e \frac{dU_e}{dx} + v \frac{\partial^2 u}{\partial y^2} - \frac{k_0}{\rho} \left[u \frac{\partial^3 u}{\partial x \partial y^2} + v \frac{\partial^3 u}{\partial y^3} + \frac{\partial u}{\partial x} \frac{\partial^2 u}{\partial y^2} - \frac{\partial u}{\partial y} \frac{\partial^2 u}{\partial x \partial y} \right] - \frac{\sigma B_0^2}{\rho} (u - u_e)$$

$$+ \frac{\pi j_0 M_0}{8\rho} \exp\left(-\frac{\pi}{a}y\right) + \frac{1}{\rho_f} \left[(1 - C_\infty) \rho_f \beta^* g(T - T_\infty) - (\rho_p - \rho_f) g(C - C_\infty) \right], \quad (2)$$

$$u \frac{\partial T}{\partial x} + v \frac{\partial T}{\partial y} = \frac{k}{\rho c_p} \left(\frac{16\sigma^{**} T_\infty^3}{3k_1} \right) \frac{\partial^2 T}{\partial y^2} + \frac{1}{(\rho c)_f} \frac{\partial}{\partial y} \left[K(T) \frac{\partial T}{\partial y} \right] + \frac{Q_0}{\rho c_p} (T - T_\infty) + \tau \left\{ D_B \left(\frac{\partial T}{\partial y} \frac{\partial C}{\partial y} \right) + \frac{D_T}{T_\infty} \left(\frac{\partial T}{\partial y} \right)^2 \right\}, \quad (3)$$

$$u \frac{\partial C}{\partial x} + v \frac{\partial C}{\partial y} = \frac{\partial}{\partial y} \left[D(C) \frac{\partial C}{\partial y} \right] + D_B \frac{\partial^2 C}{\partial y^2} + \frac{D_T}{T_\infty} \frac{\partial^2 T}{\partial y^2} - Kr^2 (C - C_\infty) \left(\frac{T}{T_\infty} \right)^n \exp\left(-\frac{E_a}{kT}\right), \quad (4)$$

$$u \frac{\partial N}{\partial x} + v \frac{\partial N}{\partial y} + \frac{bW_c}{(C_f - C_\infty)} \left[\frac{\partial}{\partial y} \left(N \frac{\partial C}{\partial y} \right) \right] = D_m \left(\frac{\partial^2 N}{\partial y^2} \right). \quad (5)$$

In expressions (3) and (4), the variable thermal conduction and concentration diffusion are [55]:

$$K(T) = k_\infty \left[1 + \lambda_1 \frac{T - T_\infty}{T_f - T_\infty} \right] \text{ and } D(C) = D_\infty \left[1 + \lambda_2 \frac{C - C_\infty}{C_\infty} \right]. \quad (6)$$

The boundary restrictions of the current flow are given by [28,50]:

$$\begin{aligned} u(x, 0) &= U_w(x) = cx, v(x, 0) = 0, -K \frac{\partial T}{\partial y} = h_f(T_f - T_\infty), \\ D_B \frac{\partial C}{\partial y} + \frac{D_T}{T_\infty} \frac{\partial T}{\partial y} &= 0, N = N_w \text{ at } y = 0, \\ u &\rightarrow U_e(x) = cx, T \rightarrow T_\infty, C \rightarrow C_\infty, N \rightarrow N_\infty \text{ as } y \rightarrow \infty. \end{aligned} \quad (7)$$

The suitable transformations are [28,50]:

$$\begin{cases} u(x, y) = cx f'(\zeta), v(x, y) = -\sqrt{cv} f(\zeta), \\ \zeta = y \sqrt{\frac{c}{v}}, \theta = \frac{T - T_\infty}{T_f - T_\infty}, \phi = \frac{C - C_\infty}{C_\infty}, \chi = \frac{N - N_\infty}{N_w - N_\infty}. \end{cases} \quad (8)$$

By implementing these transformations, governing partial differential equations are transformed into dimensionless ordinary differential equations i.e., [1,28,50,55]:

$$\begin{aligned} f''' + S^2 - (f')^2 + ff'' - We[2f'f''' - ff^{iv} - (f'')^2] + Q \exp(-\beta\zeta) - Mf' + MS + \\ B^*(\theta - Nr\phi - Nc\chi) &= 0, \end{aligned} \quad (9)$$

$$\left((1 + Rd(1 + (\theta_f - 1)\theta)^3) \theta' + \lambda_1 \theta \right) \theta'' + Prf\theta' + Pr\delta\theta + Pr(Nb\theta'\phi' + Nt\theta'^2) = 0, \quad (10)$$

$$(1 + \lambda_2 \phi) \phi'' + LePrf\phi' + \frac{Nt}{Nb} \theta'' - PrLe\sigma^*[1 + \delta_0\theta]^n \exp\left[\frac{-E}{1 + \delta_0\theta}\right] \phi = 0, \quad (11)$$

$$\chi'' + Lb(f\chi') - Pe[\phi''(\chi + \Omega) + \chi'\phi'] = 0. \quad (12)$$

The dimensionless boundary restrictions are [28,50]:

$$\begin{aligned} f'(0) &= 1, f(0) = 0, \theta'(0) = -Bi(1 - \theta(0)), \\ Nb\phi'(0) + Nt\theta'(0) &= 0, \chi(0) = 1, \end{aligned}$$

$$f'(\infty) \rightarrow S, \theta(\infty) \rightarrow 0, \phi(\infty) \rightarrow 0, \chi(\infty) \rightarrow 0. \quad (13)$$

The physical flow parameters in equations (9)-(13) are expressed by

$$\left. \begin{aligned} M &= \sqrt{\frac{\sigma \beta_0^2}{\rho c}}, Nr = \frac{(\rho_p - \rho_f)(C_\infty)}{(1-C_\infty)(T_f - T_\infty)}, S = \frac{b}{c}, We = \frac{k_0 c}{\mu_0}, \beta = \sqrt{\frac{\pi^2 v}{a^2 c}}, \\ Q &= \frac{\pi j_0 M_0}{8 \rho U_w^2}, Pr = \frac{\rho c_p}{k_\infty}, B^* = \frac{(1-C_\infty)\gamma(T_f - T_\infty)\beta^{**}}{c U_w}, Nc = \frac{\gamma g(\rho_m - \rho_f)(N_w - N_\infty)}{(1-C_\infty)(T_f - T_\infty)\beta^{**}}, \\ Nb &= \frac{\tau D_B(C_\infty)}{v}, Rd = \frac{4\sigma^{**} T_\infty^3}{k_1 k_\infty}, Nt = \frac{\tau D_T(T_f - T_\infty)}{v}, \delta = \frac{Q_0}{\rho c_p}, \\ E &= \frac{E_a}{k T_\infty}, \delta_0 = \frac{T_f - T_\infty}{T_\infty}, \sigma^* = \frac{v K r^2}{c}, Pe = \frac{b W_c}{D_m}, Lb = \frac{v}{D_m}, \Omega = \frac{N_\infty}{N_w - N_\infty}, \\ Bi &= \frac{h_f}{k_\infty} \sqrt{\frac{v}{c}}. \end{aligned} \right\} \quad (14)$$

The quantities of interest, e.g., skin coefficient C_f , Nusselt number Nu_x , Sherwood number Su_x and microorganism number Sn_x are [27,28,56]:

$$C_f = \frac{\tau_w}{\rho U_w^2}, Nu_x = \frac{x q_w}{K(T_w - T_\infty)}, Su_x = \frac{x J_w}{D_B(C_w - C_\infty)}, Sn_x = \frac{x J_n}{D_m(N_w - N_\infty)}, \quad (15)$$

where

$$\tau_w = \left[\mu_0 \frac{\partial u}{\partial y} - k_0 \left(u \frac{\partial^2 u}{\partial x \partial y} + v \frac{\partial^2 u}{\partial y^2} + 2 \frac{\partial u}{\partial x} \frac{\partial u}{\partial y} \right)^3 \right]_{y=0}, \quad (16)$$

$$q_w = -K \left(\frac{\partial T}{\partial y} \right)_{y=0}, J_w = -D_B \left(\frac{\partial C}{\partial y} \right)_{y=0}, J_n = -D_m \left(\frac{\partial N}{\partial y} \right)_{y=0}. \quad (17)$$

Hence the dimensionless forms of the above physical quantities are:

$$(Re_x)^{\frac{1}{2}} C_f = (1 - 3We) f''(0), \quad (18)$$

$$(Re_x)^{-\frac{1}{2}} Nu_x = -\theta^{(0)}, \quad (19)$$

$$Re^{-\frac{1}{2}} Su_x = -\phi'(0), \quad (20)$$

$$Re^{-\frac{1}{2}} Sn_x = -\chi'(0). \quad (21)$$

Here $Re_x = \frac{cx^2}{v}$ is the local Reynolds number.

3. Numerical approach

The coupled nonlinear dimensionless system (9)–(12) with boundary constraints (13) is solved using the Matlab bvp4c scheme for different variations of important physical prominent parameters [57–61]. The bvp4c-function is a finite-difference code that follows the three steps of Lobatto-IIIa formula. Until the process begins, problems with higher-order boundary value are converted into an initial value problem by adding several new variables. Considering

$$\left. \begin{aligned} f = q, f' = q_1, f'' = q_2, f''' = q_3, f^{iv} = q_3', \theta = q_4, \theta' = q_5, \\ \theta'' = q_5', \phi = q_6, \phi' = q_7, \phi'' = q_7', \chi = q_8, \chi' = q_9, \chi'' = q_9' \end{aligned} \right\}, \quad (22)$$

$$q_3' = \frac{-q_3 - S^2 + (q_1)^2 - qq_2 + We[2q_1q_3 - (q_2)^2] - Q \exp(-\beta\zeta) + Mq_2 - MS}{Weq}, \quad (23)$$

$$q_5' = \frac{-Prqq_5 - Pr\delta q_4 - Pr(Nbq_5q_7 + Ntq_5^2)}{\left((1+Rd(1+(\theta_f-1)q_4))^3\right)q_5 + \lambda_1q_4}, \quad (24)$$

$$q_7' = \frac{-LePrqq_7 - \frac{Nt}{Nb}q_5' + PrLe\sigma^*[1+\delta_0q_4]^n \exp\left[\frac{-E}{1+\delta_0q_4}\right]q_6}{(1+\lambda_2q_6)}, \quad (25)$$

$$q_9' = -Lb(qq_9) + Pe[q_7'(q_8 + \Omega) + q_9q_7], \quad (26)$$

with

$$\begin{aligned} q_1(0) = 1, q(0) = 0, q_5 = -Bi(1 - q_4(\zeta)), \\ Nbq_7(\zeta) + Ntq_5(\zeta) = 0, q_9(0) = 1, \text{ at } \zeta = 0, \\ q_1(\infty) = S, q_4 \rightarrow 0, q_6 \rightarrow 0, q_8 \rightarrow 0 \text{ as } \zeta \rightarrow \infty. \end{aligned} \quad (27)$$

4. Results and discussion

Significant contributions of the prominent numbers against the velocity of the Walter's B nanoliquid, thermal, concentration and micro-organism profiles are graphically demonstrated and discussed as follows:

4.1. Velocity profile

Figure 2a is constructed to display the outcomes of M and Nc against velocity f' . Velocity field f' declines when M and Nc increase. The resistive forces are upgraded with the augmentation of M ; hence, the velocity profile reduces. Basically, the magnetic number involves the Lorentz force. This resistive type of force is responsible for the decay in fluid velocity [39]. Figure 2b predicts the impacts of We and Nr against velocity profile f' . With increasing estimations of We , the velocity f' diminishes. Similarly, velocity f' shows a decreasing behavior for Nr . The modified Hartmann parameter Q and mixed convective number B^* affect the velocity of Walter's B nanofluid f' past a Riga plate, as clarified in Figure 2c. Both parameters have similar effects on velocity field f' . Figure 2d shows the impact of velocity ratio parameter S versus velocity field f' , where there is boundary layer for both $S < 0$ and $S > 0$. Velocity f' increases for larger velocity ratio parameter S . A larger velocity ratio number increases the velocity of the fluid. When the velocity ratio is zero, the usual profile at the free stream is obtained far from the plate.

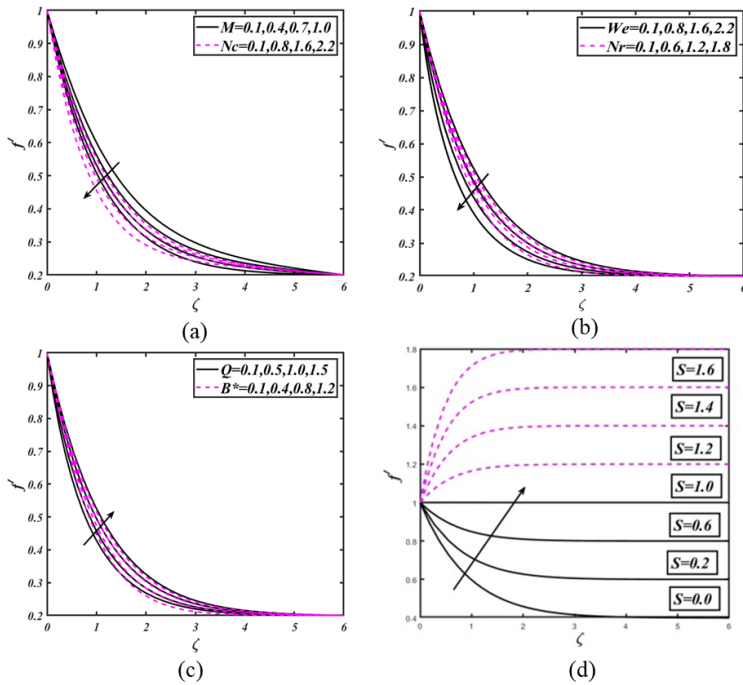


Figure 2. (a) Outcomes of f' against M & Nc ; (b) Outcomes of f' against We & Nr ; (c) Outcomes of f' against Q & B^* ; (d) Outcomes of f' against S .

4.2. Thermal profile

Figure 3a anticipates the inspiration of the Biot number Bi and thermal conductivity parameter λ_1 across the thermal field θ . Temperature θ increases for larger estimations of thermal Biot number Bi . Basically, a larger Biot number corresponds to more heat provided to the working fluid, which leads to a stronger temperature field [30]. Thermal function θ is enhanced to increase the thermal conductivity λ_1 . Figure 3b depicts the contributions of Pr and θ_f to the temperature of species θ . The thermal profile of species θ in Walter's B nanoliquid decreases with increasing estimations of Prandtl number Pr , while it increases for a larger temperature ratio parameter θ_f .

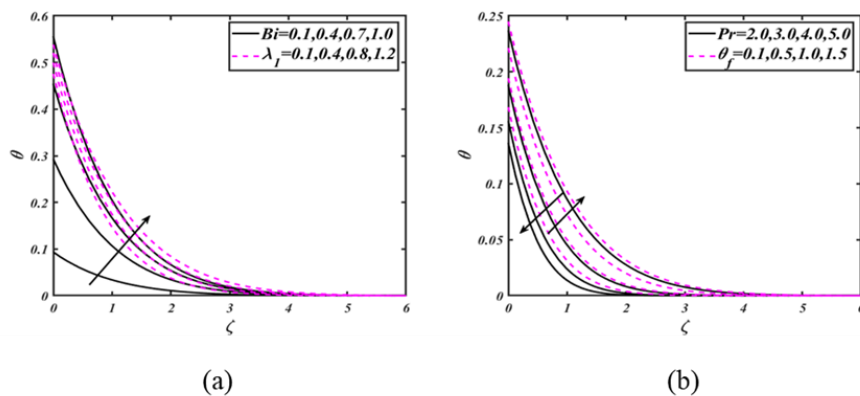


Figure 3. (a) Outcomes of θ against Bi & λ_1 ; (b) Outcomes of θ against Pr & θ_f .

4.3. Nanoparticles concentration profile

Figure 4a characterizes the impact of E and λ_2 against the nanoparticle concentration ϕ . The nanoparticle concentration ϕ increases when E increases. Furthermore, ϕ grows with larger concentration diffusivity λ_2 . Figure 4b reveals that Nt and Nb increase with the concentration of species ϕ . Here, the solutal profile of species ϕ decreases with increasing Brownian motion parameter Nb , while it increases with increasing thermophoresis parameter Nt . The natures of Pr and Le against the concentration field of species ϕ are examined in Figure 4c. Here, ϕ decreases with increasing Pr and Le .

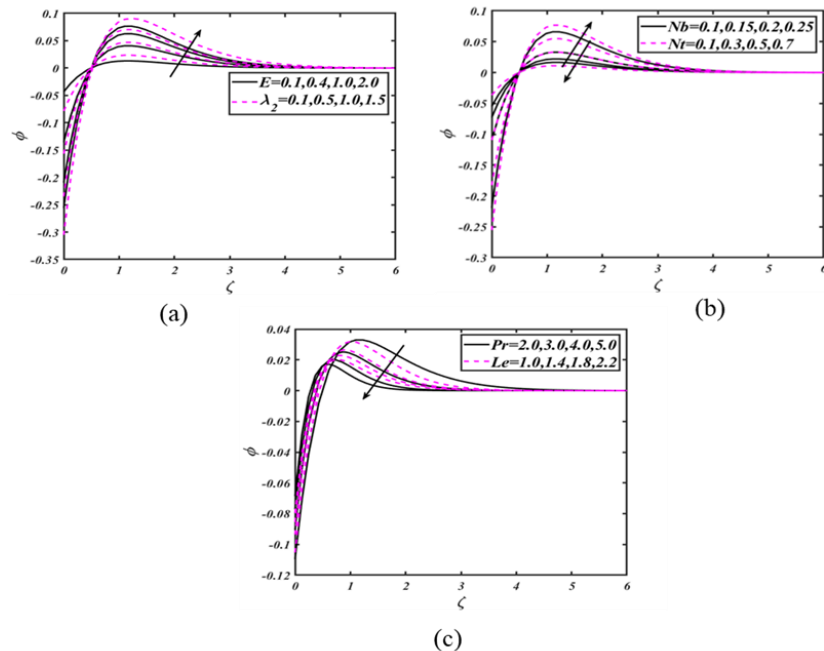


Figure 4. (a) Outcomes of ϕ against E & λ_2 ; (b) Outcomes of ϕ against Nb & Nt ; (c) Outcomes of ϕ against Pr & Le .

4.4. Microorganism profile

Figure 5 examines the outcome of bioconvection Lewis parameter Lb and Peclet parameter Pe versus the microorganism field χ . The microorganism field χ decreases with higher estimations of both parameters Lb and Pe .

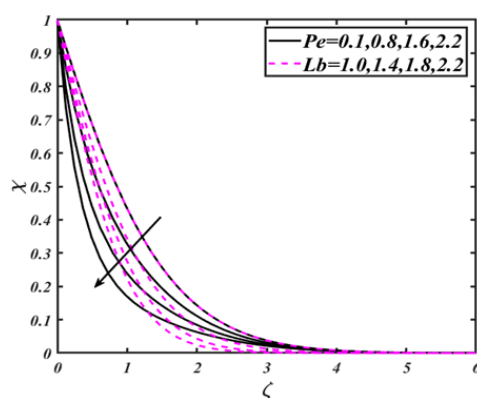


Figure 5. Outcomes of χ against Pe & Lb .

4.5. Tabular data

Tables 1–4 are captured to check the behaviors of skin friction $-f''(0)$, Nusselt $-\theta'(0)$, Sherwood $-\phi'(0)$ and microorganism $-\chi'(0)$ numbers versus various interesting parameters. Table 1 displays the contribution of $-f''(0)$ versus B^*, Q, M, Nr and Nc . Here $-f''(0)$ decays by augmenting estimations of B^* , Q and M . Table 2 compares $f''(0)$ for varying B^* with Ahmad et al. [27]. Here, we found agreement between the presented bvp4c solution and the shooting solution in Ahmad et al. [27] in the limiting case. Table 3 shows the contribution of $-\theta'(0)$ versus $Pr, Nb, Nt, Le, M, Bi, B^*, Nr$ and Nc . We note that $-\theta'(0)$ increases as Nb and Pr are increased. In Table 4, $-\phi'(0)$ decreases for Le and increases for larger Nt . Table 5 shows that $-\chi'(0)$ decreases for Pe and Lb .

Table 1. Comparative outcomes of $-f''(0)$ for variations of B^*, Q, M, Nr and Nc .

B^*	Q	M	Nr	Nc	$-f''(0)$
0.1					0.6271
0.8	2.0	0.5	0.1	0.2	0.5301
1.6					0.4249
	1.0				0.6243
0.2	1.6	0.5	0.2	0.2	0.6176
	2.2				0.6059
	0.1				0.4912
0.2	2.0	0.6	0.2	0.2	0.6384
	1.2				0.7657
	0.1				0.6123
0.2	2.0	0.5	1.0	0.2	0.6174
	2.0				0.6243
	0.1				0.6098
0.2	2.0	0.5	0.1	1.0	0.6360
	2.0				0.6697

Table 2. Outcomes of $f''(0)$ for variations of B^* when $Q = 0.5, Pr = 5, \beta = 0.5, Bi = 50, Nt = 0.5, Nb = 0.5, Nr = 0.1, LePr = 0.5, S = 1$ and $We = Nc = M = 0$.

B^*	Ahmad et al. [27]	Present results
0	1.5394682	1.5394732
1	1.9023442	1.9023488
2	2.2416224	2.2416273
3	2.5631502	2.5631452
4	2.8705968	2.8706019

Table 3. Outcomes of $-\theta'(0)$ for variations of Pr , Nb , Nt , Le , M , Bi , B^* , Nr and Nc .

Pr	Nb	Nt	Le	M	Bi	B^*	Nr	Nc	$-\theta'(0)$
2	0.2	0.3	2.0	0.5	2.0	0.2	0.2	0.2	0.7709
3									0.8729
4									0.9450
1.2	0.1	0.3	2.0	0.5	2.0	0.2	0.2	0.2	0.6454
	0.5								0.6456
	1.0								0.6457
1.2	0.2	0.1	2.0	0.5	2.0	0.2	0.2	0.2	0.6518
	0.5								0.6394
	1.0								0.6240
1.2	0.2	0.3	1.0	0.5	2.0	0.2	0.2	0.2	0.6481
			1.8						0.6460
			2.6						0.6445
1.2	0.2	0.3	2.0	0.1	2.0	0.2	0.2	0.2	0.6566
				0.6					0.6444
				1.2					0.6336
1.2	0.2	0.3	2.0	0.5	0.3	0.2	0.2	0.2	0.2299
					1.0				0.4898
					1.8				0.6245
1.2	0.2	0.3	2.0	0.5	2.0	0.1	0.2	0.2	0.6456
						0.8			0.6525
						1.6			0.6594
1.2	0.2	0.3	2.0	0.5	2.0	0.2	0.1	0.2	0.6468
							1.0		0.6460
							2.0		0.6452
1.2	0.2	0.3	2.0	0.5	2.0	0.2	0.2	0.1	0.6468
								1.0	0.6453
								2.0	0.6434

Table 4. Outcomes of $-\phi'(0)$ for variations of Pr , Nb , Nt , Le , M , B^* , Bi , Nr and Nc .

Pr	Nb	Nt	Le	M	B^*	Bi	Nr	Nc	$-\phi'(0)$
2	0.2	0.3	2.0	0.5	2.0	0.5	0.2	0.2	1.1564
3									1.3094
4									1.4175
1.2	0.1	0.3	2.0	0.5	2.0	0.5	0.2	0.2	1.9363
	0.5								0.3874
	1.0								0.1937
1.2	0.2	0.1	2.0	0.5	2.0	0.5	0.2	0.2	0.3259
			0.5						1.5984
			1.0						3.1199

Continued on next page

Pr	Nb	Nt	Le	M	B^*	Bi	Nr	Nc	$-\phi'(0)$
1.2	0.2	0.3	1.0	0.5	2.0	0.5	0.2	0.2	0.9721
									0.9690
									0.9668
1.2	0.2	0.3	2.0	0.1	2.0	0.5	0.2	0.2	0.9849
									0.9585
									0.9503
1.2	0.2	0.3	2.0	0.5	0.1	0.5	0.2	0.2	0.9684
									0.9788
									0.9892
1.2	0.2	0.3	2.0	0.5	2.0	0.1	0.2	0.2	0.3434
									0.7346
									0.9367
1.2	0.2	0.3	2.0	0.5	2.0	0.5	0.1	0.2	0.9701
									0.9691
									0.9679
1.2	0.2	0.3	2.0	0.5	2.0	0.5	0.2	0.1	0.9703
									0.9679
									0.9652

Table 5. Outcomes of $-\chi'(0)$ for variations of Pe , Lb , M , Nr and Nc .

Pe	Lb	M	Nr	Nc	$-\chi'(0)$
0.1	2.0	0.5	0.1	0.2	1.0873
					1.7010
					2.4250
0.6	1.0	0.5	0.2	0.2	1.1303
					1.3814
					1.1546
0.6	2.0	0.1	0.2	0.2	1.4608
					1.4302
					1.4029
0.6	2.0	0.5	0.1	0.2	1.4358
					1.4340
					1.4320
0.6	2.0	0.5	0.1	0.1	1.4360
					1.4318
					1.4270

5. Conclusions

The current work discusses the bioconvection nonlinear flow of Walter's B nanoliquid over a Riga plate with variable thermal conduction and concentration diffusion features. The aspects of thermal radiation and activation energy are considered. First, the coupled partial differential equations are embedded into the dimensionless system of nonlinear ODEs through suitable transformations [62–65]. The achieved dimensionless system of ODEs is solved by using the MATLAB built-in bvp4c solver,

which follows the Lobatto-IIIa formula. The main results of the considered problem are summarized below.

- Velocity has an enlarging effect for higher estimations of mixed convection and modified Hartmann numbers.
- The temperature of Walter's B nanoliquid increases via larger estimations of Biot number and thermal conductivity parameter.
- The nanoparticle concentration is improved for larger concentration diffusion and activation energy parameters.
- Microorganism fields have similar features for both Peclet and microorganism Lewis parameters.
- The current bioconvective nonlinear Walter's B nanoliquid model has a significant role in the power generation, medical sciences, energy manufacturing, metallurgical industry, thermal recovery of oil, heat storage devices, etc. [66–70].

Acknowledgment

The authors extend their appreciation to the Deanship of Scientific Research at King Khalid University, Abha, Saudi Arabia for funding this work through Large Groups Project under grant number RGP.2/206/43.

Conflict of interest

The author declares no conflict of interest.

References

1. K. Walters, Non-newtonian effects in some elastic-viscous liquids whose behaviour at small rates of shear is characterized by a general linear equation of state, *Quart. J. Mech. Appl. Math.*, **15** (1962), 63–76. <https://doi.org/10.1093/qjmam/15.1.63>
2. M. M. Nandeppanavar, M. S. Abel, J. Tawade, Heat transfer in a Walter's liquid B fluid over an impermeable stretching sheet with non-uniform heat source/sink and elastic deformation, *Commun. Nonlinear Sci. Numer. Simul.*, **15** (2010), 1791–1802. <https://doi.org/10.1016/j.cnsns.2009.07.009>
3. S. Nadeem, R. Mehmood, S. S. Motsa, Numerical investigation on MHD oblique flow of a Walter's B type nano fluid over a convective surface, *Int. J. Therm. Sci.*, **92** (2015), 162–172. <https://doi.org/10.1016/j.ijthermalsci.2015.01.034>
4. T. Hayat, S. Qayyum, M. Imtiaz, A. Alsaedi, Radiative Falkner-Skan flow of Walter-B fluid with prescribed surface heat flux, *J. Theor. Appl. Mech.*, **55** (2017), 117–127. <https://doi.org/10.15632/jtam-pl.55.1.117>
5. A. Majeed, T. Javed, S. Shami, Numerical analysis of Walters-B fluid flow and heat transfer over a stretching cylinder, *Can. J. Phys.*, **94** (2016), 522–530. <https://doi.org/10.1139/cjp-2015-0511>
6. T. Hayat, S. Asad, M. Mustafa, H. H. Alsulami, Heat transfer analysis in the flow of Walters' B fluid with a convective boundary condition, *Chinese Phys. B*, **23** (2014), 084701. <https://doi.org/10.1088/1674-1056/23/8/084701>

7. M. Ijaz, M. Yousaf, A. M. El Shafey, Arrhenius activation energy and Joule heating for Walter–B fluid with Cattaneo–Christov double-diffusion model, *J. Therm. Anal. Calorim.*, **143** (2021), 3687–3698. <https://doi.org/10.1007/s10973-020-09270-1>
8. K. Loganathan, N. Nithyadevi, P. Boopathi, K. Mohana, Inquiry of inclined magnetic field effects on Walter–B nanofluid flow with heat generation/absorption, *IOP Conf. Ser.: Mater. Sci. Eng.*, **872** (2020), 012097. <https://doi.org/10.1088/1757-899X/872/1/012097>
9. M. Mueller, O. A. Igbokwe, B. Walter, C. L. Pederson, S. Riechelmann, D. K. Richter, et al., Testing the preservation potential of early diagenetic dolomites as geochemical archives, *Sedimentology*, **67** (2020), 849–881. <https://doi.org/10.1111/sed.12664>
10. B. Meier, A. Schmidt, N. Glaser, A. Meining, B. Walter, A. Wannhoff, et al., Endoscopic full-thickness resection of gastric subepithelial tumors with the gFTRD-system: A prospective pilot study (RESET trial), *Surg. Endosc.*, **34** (2020), 853–860. <https://doi.org/10.1007/s00464-019-06839-2>
11. S. U. S. Choi, J. A. Eastman, Enhancing thermal conductivity of fluids with nanoparticles, *ASME Pub Fed.*, **231** (1995), 99–106.
12. J. Buongiorno, Convective transport in nanofuids, *J. Heat Transfer*, **128** (2006), 240–250. <https://doi.org/10.1115/1.2150834>
13. K. L. Hsiao, Stagnation electrical MHD nanofuid mixed convection with slip boundary on a stretching sheet, *Appl. Therm. Eng.*, **98** (2016), 850–861. <https://doi.org/10.1016/j.applthermaleng.2015.12.138>
14. M. M. Rashidi, N. Freidoonimehr, A. Hosseini, O. A. Beg, T. K. Hung, Homotopy simulation of nanofuid dynamics from a non-linearly stretching isothermal permeable sheet with transpiration, *Meccanica*, **49** (2014), 469–482. <https://doi.org/10.1007/s11012-013-9805-9>
15. M. Sheikholeslami, M. M. Bhatti, Forced convection of nanofluid in presence of constant magnetic field considering shape effects of nanoparticles, *Int. J. Heat Mass Tran.*, **111** (2017), 1039–1049. <https://doi.org/10.1016/j.ijheatmasstransfer.2017.04.070>
16. M. Turkyilmazoglu, Condensation of laminar film over curved vertical walls using single and two-phase nanofluid models, *Eur. J. Mech.-B/Fluids*, **65** (2017), 184–191. <https://doi.org/10.1016/j.euromechflu.2017.04.007>
17. R. Ellahi, *Recent developments of nanofluids*, MDPI-Multidisciplinary Digital Publishing Institute, 2018. <https://doi.org/10.3390/books978-3-03842-834-3>
18. A. Pantokratoras, Discussion:“Computational analysis for mixed convective flows of viscous fluids with nanoparticles”(Farooq, U., Lu, DC, Ahmed, S., and Ramzan, M., 2019, ASME J. Therm. Sci. Eng. Appl., 11(2), p. 021013), *J. Thermal. Sci. Eng. Appl.*, **11** (2019), 055503. <https://doi.org/10.1115/1.4043092>
19. M. Rashid, A. Alsaedi, T. Hayat, B. Ahmed, Magnetohydrodynamic flow of Maxwell nanofluid with binary chemical reaction and Arrhenius activation energy, *Appl. Nanosci.*, **10** (2020), 2951–2963. <https://doi.org/10.1007/s13204-019-01143-w>
20. T. Tayebi, A. J. Chamkha, Magnetohydrodynamic natural convection heat transfer of hybrid nanofluid in a square enclosure in the presence of a wavy circular conductive cylinder, *J. Therm. Sci. Eng. Appl.*, **12** (2020), 031009. <https://doi.org/10.1115/1.4044857>
21. T. Hayat, R. Riaz, A. Aziz, A. Alsaedi, Influence of Arrhenius activation energy in MHD flow of third grade nanofluid over a nonlinear stretching surface with convective heat and mass conditions, *Physica A*, **549** (2020), 124006. <https://doi.org/10.1016/j.physa.2019.124006>

22. T. Muhammad, H. Waqas, S. A. Khan, R. Ellahi, S. M. Sait, Significance of nonlinear thermal radiation in 3D Eyring–Powell nanofluid flow with Arrhenius activation energy, *J. Therm. Anal. Calorim.*, **143** (2021), 929–944. <https://doi.org/10.1007/s10973-020-09459-4>
23. S. Z. Alamri, R. Ellahi, N. Shehzad, A. Zeeshan, Convective radiative plane Poiseuille flow of nanofluid through porous medium with slip: An application of Stefan blowing, *J. Mol. Liq.*, **273** (2019), 292–304. <https://doi.org/10.1016/j.molliq.2018.10.038>
24. I. Khan, A. Hussain, M. Y. Malik, S. Mukhtar, On magnetohydrodynamics Prandtl fluid flow in the presence of stratification and heat generation, *Physica A*, **540** (2020), 123008. <https://doi.org/10.1016/j.physa.2019.123008>
25. S. E. Awan, M. A. Z. Raja, A. Mehmood, S. A. Niazi, S. Siddiq, Numerical treatments to analyze the nonlinear radiative heat transfer in MHD nanofluid flow with solar energy, *Arab. J. Sci. Eng.*, **45** (2020), 4975–4994. <https://doi.org/10.1007/s13369-020-04593-5>
26. A. Gailitis, O. Lielausis, On a possibility to reduce the hydrodynamic resistance of a plate in an electrolyte, *Appl. Magnetohydrodynamics Rep. Inst. Riga*, **13** (1961), 143–146.
27. R. Ahmad, M. Mustafa, M. Turkyilmazoglu, Buoyancy effects on nanofluid flow past a convectively heated vertical Riga-plate: A numerical study, *Int. J. Heat Mass Tran.*, **111** (2017), 827–835. <https://doi.org/10.1016/j.ijheatmasstransfer.2017.04.046>
28. Z. Iqbal, Z. Mehmood, E. Azhar, E. N. Maraj, Numerical investigation of nanofluid transport of gyrotactic microorganisms submerged in water towards Riga plate, *J. Mol. Liq.*, **234** (2017), 296–308. <https://doi.org/10.1016/j.molliq.2017.03.074>
29. R. Ellahi, M. Hassan, A. Zeeshan, Aggregation effects on water base Al_2O_3 -nanofluid over permeable wedge in mixed convection, *Asia-Pac. J. Chem. Eng.*, **11** (2016), 179–186. <https://doi.org/10.1002/apj.1954>
30. R. M. Kasmani, S. Sivasankaran, M. Bhuvaneswari, Z. Siri, Effect of chemical reaction on convective heat transfer of boundary layer flow in nanofluid over a wedge with heat generation/absorption and suction, *J. Appl. Fluid Mech.*, **9** (2015), 379–388. <https://doi.org/10.18869/acadpub.jafm.68.224.24151>
31. M. Khan, M. Azam, A. S. Alshomrani, Effects of melting and heat generation/absorption on unsteady Falkner-Skan flow of Carreau nanofluid over a wedge, *Int. J. Heat Mass Tran.*, **110** (2017), 437–446. <https://doi.org/10.1016/j.ijheatmasstransfer.2017.03.037>
32. A. K. Pandey, M. Kumar, Chemical reaction and thermal radiation effects on a boundary layer flow of nanofluid over a wedge with viscous and Ohmic dissipation, *St. Petersburg Polytechnical Univ. J.: Phys. Math.*, **3** (2017), 322–332. <https://doi.org/10.1016/j.spjpm.2017.10.008>
33. M. Khan, M. Azam, A. S. Alshomrani, Unsteady slip flow of Carreau nanofluid over a wedge with nonlinear radiation and new mass flux condition, *Res. Phys.*, **7** (2017), 2261–2270. <https://doi.org/10.1016/j.rinp.2017.06.038>
34. A. Chamkha, S. Abbasbandy, A. M. Rashad, Non-Darcy natural convection flow for non-Newtonian nanofluid over cone saturated in porous medium with uniform heat and volume fraction fluxes, *Int. J. Numer. Method. Heat Fluid Flow*, **25** (2015), 422–437. <https://doi.org/10.1108/HFF-02-2014-0027>
35. M. Macha, N. Kishan, Boundary layer flow of viscoelastic nanofluid over a wedge in the presence of buoyancy force effects, *Comput. Therm. Sci.: An Int. J.*, **9** (2017), 257–267. <https://doi.org/10.1615/ComputThermalScien.2017016742>

36. A. V. Kuznetsov, Thermo bioconvection in a suspension of oxytactic bacteria, *Int. Commun. Heat Mass Tran.*, **32** (2005), 991–999. <https://doi.org/10.1016/j.icheatmasstransfer.2004.11.005>
37. Y. R. Li, H. Waqas, M. Imran, U. Farooq, F. Mallawi, I. Tlili, A numerical exploration of modified second-grade nanofluid with motile microorganisms, thermal radiation, and Wu's slip, *Symmetry*, **12** (2020), 393. <https://doi.org/10.3390/sym12030393>
38. T. Muhammad, S. Z. Alamri, H. Waqas, D. Habib, R. Ellahi, Bioconvection flow of magnetized Carreau nanofluid under the influence of slip over a wedge with motile microorganisms, *J. Therm. Anal. Calorim.*, **143** (2021), 945–957. <https://doi.org/10.1007/s10973-020-09580-4>
39. S. U. Khan, H. Waqas, M. M. Bhatti, M. Imran, Bioconvection in the rheology of magnetized couple stress nanofluid featuring activation energy and Wu's slip, *J. Non-Equil. Thermody.*, **45** (2020), 81–95. <https://doi.org/10.1515/jnet-2019-0049>
40. T. P. Zhang, S. U. Khan, M. Imran, I. Tlili, H. Waqas, N. Ali, Activation energy and thermal radiation aspects in bioconvection flow of rate type nanoparticles configured by a stretching/shrinking disk, *J. Energy Resour. Technol.*, **142** (2020), 112102. <https://doi.org/10.1115/1.4047249>
41. H. Waqas, M. Imran, T. Muhammad, S. M. Sait, R. Ellahi, Numerical investigation on bioconvection flow of Oldroyd-B nanofluid with nonlinear thermal radiation and motile microorganisms over rotating disk, *J. Therm. Anal. Calorim.*, **145** (2021), 523–539. <https://doi.org/10.1007/s10973-020-09728-2>
42. N. S. Khan, Q. Shah, A. Bhaumik, P. Kumam, P. Thounthong, I. Amiri, Entropy generation in bioconvection nanofluid flow between two stretchable rotating disks, *Sci. Rep.*, **10** (2020), 4448. <https://doi.org/10.1038/s41598-020-61172-2>
43. S. U. Mamatha, K. R. Babu, P. D. Prasad, C. S. K. Raju, S. V. K. Varma, Mass transfer analysis of two-phase flow in a suspension of microorganisms, *Arch. Thermodyn.*, **41** (2020), 175–192. <https://doi.org/10.24425/ather.2020.132954>
44. M. Ferdows, M. G. Reddy, F. Alzahrani, S. Y. Sun, Heat and mass transfer in a viscous nanofluid containing a gyrotactic micro-organism over a stretching cylinder, *Symmetry*, **11** (2019), 1131. <https://doi.org/10.3390/sym11091131>
45. N. A. Amirsom, M. J. Uddin, M. F. M. Basir, A. Ismail, O. A. Beg, A. Kadir, Three-dimensional bioconvection nanofluid flow from a bi-axial stretching sheet with anisotropic slip, *Sains Malays.*, **48** (2019), 1137–1149. <http://doi.org/10.17576/jsm-2019-4805-23>
46. S. Kasaragadda, I. M. Alarifi, M. Rahimi-Gorji, R. Asmatulu, Investigating the effects of surface superhydrophobicity on moisture ingressions of nanofiber-reinforced bio-composite structures, *Microsyst. Technol.*, **26** (2020), 447–459. <https://doi.org/10.1007/s00542-019-04507-y>
47. M. S. Ansari, O. Otegbeye, M. Trivedi, S. P. Goqo, Magnetohydrodynamic bio-convective Casson nanofluid flow: A numerical simulation by paired quasilinearisation, *J. Appl. Comput. Mech.*, **7** (2021), 2024–2039. <https://doi.org/10.22055/JACM.2020.31205.1839>
48. M. S. Alqarni, S. Yasmin, H. Waqas, S. A. Khan, Recent progress in melting heat phenomenon for bioconvection transport of nanofluid through a lubricated surface with swimming microorganisms, *Sci. Rep.*, **12** (2022), 8447. <https://doi.org/10.1038/s41598-022-12230-4>
49. S. M. H. Zadeh, S. A. M. Mehryan, M. A. Sheremet, M. Izadi, M. Ghodrat, Numerical study of mixed bio-convection associated with a micropolar fluid, *Therm. Sci. Eng. Prog.*, **18** (2020), 100539. <https://doi.org/10.1016/j.tsep.2020.100539>

50. M. M. Bhatti, E. E. Michaelides, Study of Arrhenius activation energy on the thermo-bioconvection nanofluid flow over a Riga plate, *J. Therm. Anal. Calorim.*, **143** (2021), 2029–2038. <https://doi.org/10.1007/s10973-020-09492-3>
51. H. Waqas, S. U. Khan, M. Imran, M. M. Bhatti, Thermally developed Falkner–Skan bioconvection flow of a magnetized nanofluid in the presence of a motile gyrotactic microorganism: Buongiorno’s nanofluid model, *Phys. Scr.*, **94** (2019), 115304. <https://doi.org/10.1088/1402-4896/ab2ddc>
52. A. M. Alwatban, S. U. Khan, H. Waqas, I. Tlili, Interaction of Wu’s slip features in bioconvection of Eyring Powell nanoparticles with activation energy, *Processes*, **7** (2019), 859. <https://doi.org/10.3390/pr7110859>
53. Y. Wang, H. Waqas, M. Tahir, M. Imran, C. Y. Jung, Effective Prandtl aspects on bio-convective thermally developed magnetized tangent hyperbolic nanoliquid with Gyrotactic microorganisms and second order velocity slip, *IEEE Access*, **7** (2019), 130008–130023. <https://doi.org/10.1109/ACCESS.2019.2940203>
54. M. Z. Ullah, T. S. Jang, An efficient numerical scheme for analyzing bioconvection in von-Kármán flow of third-grade nanofluid with motile microorganisms, *Alex. Eng. J.*, **59** (2020), 2739–2752. <https://doi.org/10.1016/j.aej.2020.05.017>
55. A. S. Alshomrani, M. Z. Ullah, D. Baleanu, Importance of multiple slips on bioconvection flow of cross nanofluid past a wedge with gyrotactic motile microorganisms, *Case Stud. Therm. Eng.*, **22** (2020), 100798. <https://doi.org/10.1016/j.csite.2020.100798>
56. A. Shafiq, Z. Hammouch, A. Turab, Impact of radiation in a stagnation point flow of Walters’ B fluid towards a Riga plate, *Therm. Sci. Eng. Prog.*, **6** (2018), 27–33. <https://doi.org/10.1016/j.tsep.2017.11.005>
57. M. M. Peiravi, J. Alinejad, D. Ganji, S. Maddah, Numerical study of fins arrangement and nanofluids effects on three-dimensional natural convection in the cubical enclosure, *Chall. Nano Micro Scale Sci. Technol.*, **7** (2019), 97–112. <https://doi.org/10.22111/tpnms.2019.4845>
58. M. M. Peiravi, J. Alinejad, Hybrid conduction, convection and radiation heat transfer simulation in a channel with rectangular cylinder, *J. Therm. Anal. Calorim.*, **140** (2020), 2733–2747. <https://doi.org/10.1007/s10973-019-09010-0>
59. J. Alinejad, M. M. Peiravi, Numerical analysis of secondary droplets characteristics due to drop impacting on 3D cylinders considering dynamic contact angle, *Meccanica*, **55** (2020), 1975–2002. <https://doi.org/10.1007/s11012-020-01240-z>
60. M. M. Peiravi, J. Alinejad, D. D. Ganji, S. Maddah, 3D optimization of baffle arrangement in a multi-phase nanofluid natural convection based on numerical simulation, *Int. J. Numer. Method. Heat Fluid Flow*, **30** (2020), 2583–2605. <https://doi.org/10.1108/HFF-01-2019-0012>
61. M. M. Peiravi, J. Alinejad, Nano particles distribution characteristics in multi-phase heat transfer between 3D cubical enclosures mounted obstacles, *Alex. Eng. J.*, **60** (2021), 5025–5038. <https://doi.org/10.1016/j.aej.2021.04.013>
62. J. K. Madhukesh, A. Alhadhrami, R. N. Kumar, R. J. P. Gowda, B. C. Prasannakumara, R. S. V. Kumar, Physical insights into the heat and mass transfer in Casson hybrid nanofluid flow induced by a Riga plate with thermophoretic particle deposition, *P. I. Mech. Eng. Part E: J. Proc. Mech. Eng.*, 2021, <https://doi.org/10.1177/09544089211039305>

63. J. K. Madhukesh, R. S. V. Kumar, R. J. P. Gowda, B. C. Prasannakumara, S. A. Shehzad, Thermophoretic particle deposition and heat generation analysis of Newtonian nanofluid flow through magnetized Riga plate, *Heat Transf.*, **51** (2022), 3082–3098. <https://doi.org/10.1002/htj.22438>
64. R. J. P. Gowda, R. N. Kumar, A. M. Jyothi, B. C. Prasannakumara, I. E. Sarris, Impact of binary chemical reaction and activation energy on heat and mass transfer of Marangoni driven boundary layer flow of a non-Newtonian nanofluid, *Processes*, **9** (2021), 702. <https://doi.org/10.3390/pr9040702>
65. A. M. Jyothi, R. N. Kumar, R. J. P. Gowda, Y. Veeranna, B. C. Prasannakumara, Impact of activation energy and gyrotactic microorganisms on flow of Casson hybrid nanofluid over a rotating moving disk, *Heat Transf.*, **50** (2021), 5380–5399. <https://doi.org/10.1002/htj.22129>
66. B. Shaker, M. Gholinia, M. Pourfallah, D. D. Ganji, CFD analysis of Al_2O_3 -syltherm oil Nanofluid on parabolic trough solar collector with a new flange-shaped turbulator model, *Theor. Appl. Mech. Lett.*, **12** (2022), 100323. <https://doi.org/10.1016/j.taml.2022.100323>
67. F. H. Sani, M. Pourfallah, M. Gholinia, The effect of MoS_2 –Ag/H₂O hybrid nanofluid on improving the performance of a solar collector by placing wavy strips in the absorber tube, *Case Stud. Therm. Eng.*, **30** (2022), 101760. <https://doi.org/10.1016/j.csite.2022.101760>
68. A. H. Ghobadi, M. G. Hassankolaei, A numerical approach for MHD Al_2O_3 – TiO_2 /H₂O hybrid nanofluids over a stretching cylinder under the impact of shape factor, *Heat Transf.*, **48** (2019), 4262–4282. <https://doi.org/10.1002/htj.21591>
69. S. Shahlaei, M. G. Hassankolaei, MHD boundary layer of GO–H₂O nanoliquid flow upon stretching plate with considering nonlinear thermal ray and Joule heating effect, *Heat Transf.*, **48** (2019), 4152–4173. <https://doi.org/10.1002/htj.21586>
70. A. H. Ghobadi, M. G. Hassankolaei, Numerical treatment of magneto Carreau nanofluid over a stretching sheet considering Joule heating impact and nonlinear thermal ray, *Heat Transf.*, **48** (2019), 4133–4151. <https://doi.org/10.1002/htj.21585>



AIMS Press

© 2022 the Author(s), licensee AIMS Press. This is an open access article distributed under the terms of the Creative Commons Attribution License (<http://creativecommons.org/licenses/by/4.0>)